Bull. Inst. Zool., Academia Sinica **32**(1): 39-53 (1993)

Histomorphology of the neurosecretory system in the Indian white prawn *Penaeus indicus* H. Milne Edwards

K. SUNILKUMAR MOHAMED, K.K. VIJAYAN and A.D. DIWAN

Central Marine Fisheries Research Institute,
P.B. 2704, Dr. Salim
Ali Road, Kochi 682 031, Kerala State, India

(Accepted May 13, 1992)

The neurosecretory system of the Indian white prawn, *Penaeus indicus* was examined under light and transmission electron microscopy. Four morphological types of neurosecretory cells were identified: GN (giant neuron), A, B, and C. The characteristics of these cells, together with their histochemical properties, are described. All neurosecretory cells displayed cyclic secretory activity, and – based on the presence of stainable granules, vacuoles and glial cells – three secretory cycle phases were noted. The distribution of the neurosecretory cell groups in the eyestalk and brain, plus the tritocerebral, subesophageal, thoracic and abdominal ganglia are described and mapped. GN cells were absent from the X-organs of the eyestalk, but they dominated in all the other ganglia. Neurosecretory material was found to be haloed dense core granules with diameters between 1400 and 1600 Å.

Key words: Neurosecretory cell types, secretory phases and distribution, *Penaeus indicus*.

Several physiological functions of crustraceans, such as reproduction and growth, are known to be under the control of neuroendocrine hormones (Adiyodi and Adiyodi, 1970). Therefore, information on the neurosecretory cells (NSCs) which produce these hormones is required to successfully manipulate the life cycle of penaeid prawns in aquaculture. Nevertheless, investigations on penaeid neurosecretion are limited, with the earliest study being that of Dall (1965) on the neuroendocrine centers of the Australian school prawn *Metapenaeus* sp. Neurosecretion in the Japanese shrimp *Penaeus japonicus* was studied by Nakamura (1974), and NSCs in *P. monodon* and *Parapenaeopsis stylifera* were breifly described by Nanda and Ghosh (1985) and Nagabhushanam *et al.* (1986), respectively. However, none of these studies dealt fully with the morphology of the neurosecretory system, NSC types, and their secretory cycles, nor did they map NSCs in different ganglia. Furthermore, among penaeids, there have been very few histochemical and ultrastructural studies on the NSCs, and hence their chemical nature and structural details are not fully understood.

The present study therefore describes in detail the neurosecretory system of *Penaeus indicus,* including cell types, distribution, mapping, histochemical nature of the neurosecretory products, and the cyclic secretory activities of these cells.

MATERIALS AND METHODS

Live *P. indicus* adults ranging from 120-170 mm total length were collected off the

coast of Kochi using short duration otter trawls. The prawns were then transported directly to the laboratory for use in this study.

To investigate the animal's neurosecretory system, all ganglionic masses (including the eyestalk) were excised from freshly sacrificed prawns and fixed in Bouin's fluid for 24-48 h before being processed for histological studies. Sections of processed tissue (6-8 μm thick) were stained using Gomori's paraldehyde fuchsin method (Kurup, 1972) for observing the NSCs. Photomicrographs were taken using an Olympus research microscope. For mapping NSCs in different ganglia, a series of sections were observed, and the positions of NSC groups were then reconstructed diagrammatically.

Histochemical tests for detecting proteins, carbohydrates, and nucleic acids were performed with ganglia that had been fixed in 10% neutral buffered formalin for 24-48 h. For lipid histochemistry, thick sections of frozen ganglia (10 μm) were cut using a Histostat. Tests for detecting general proteins, amino groups, sulphydryl groups, disulphide groups, glycogen, mucopolysaccharides, RNA, DNA, and lipids were carried out with suitable controls according to Pearse (1968).

Ultrastructural investigations on neurosecretory material were performed on the X-organ complexes of eyestalks; eyestalks were fixed in 4% gluteraldehyde and processed for ultramicrotomy. Uranyl acetate- and Lead citrate-stained ultrathin sections were observed using a JEOL-JEM 100 CX II electron microscope.

RESULTS

Based on their affinity for aldehyde fuchsin stain, neurosecretory cells were identified in the optic (eyestalk), supraesophageal (brain), tritocerebral, subesophageal, thoracic, and abdominal ganglia. Histologically, *P. indicus* NSCs were found to be different from the multitude of non-neurosecretory neurons present in the ganglia; they were characterized by the presence of large nuclei, abundant cytoplasm, and conspicuous granules in their perikarya. All NSCs were unipolar and non-dendritic; nevertheless, they differed significantly in size, shape, and secretory activity. On the basis of these characters, the observed NSCs were arbitrarily classified into four types: giant neurons (GN) and types A, B, and C cells (Table 1).

Giant Neuron (GN)

These modified neurons were the largest NSCs observed; they are oval to polygonal in shape, with a centrally placed vesicular nucleus (Fig. 1). Nucleoli were dispersed in the karyoplasm, their numbers ranging from eight to ten. All GN cells were observed to be rich in cytoplasm, as evidenced by a low nucleus-cytoplasm ratio (Table 1). Perinuclear vacuoles and pericellular capillary plexus and glial cells were also observed. Histochemical tests showed that the cells were generally rich in proteins (mainly cystine) and glycogen, and had small amounts of lipids and nucleic acids (Table 2).

A cells

These cells were smaller than GN cells, but had the same shape (Table 1). Type A cells possessed centrally-placed nuclei and two-to-four nucleoli in the karyoplasm (Fig. 1). Vacuoles were observed in the peripheral regions of A cells; glial cells and capillary plexuses were also observed in the pericellular regions circumscribing these cells. The perikarya showed strong positive reactions to tests for sulphur-containing amino acids and glycogen. Each A cell's cytoplasm contained only moderate quantities of lipids, and was poor in RNA (Table 2).

Table 1. Cell and nucleus diameters and distribution of NSC in *P. indicus.*

Cell type	Cell diameter ($\mu \pm SD$)	Nucleus diameter ($\mu \pm SD$)	Nucleus cytoplasm Ratio Range	Distribution
GN Cells (Giant Neuron)	75 ± 12	27 ± 5	0.3 – 0.4	Supraesophageal, Subesophageal, Thoracic, and Tritocerebral ganglia.
A Cells (Large Oval Cells)	40 ± 7	15 ± 6	0.3 – 0.5	Eyestalk, CNS
B Cells (Small Oval Cells)	23 ± 4	10 ± 3	0.4 – 0.6	Eyestalk, CNS
C Cells (Pyriform Cells)	15 ± 4	9 ± 3	0.4 – 0.7	Eyestalk, CNS (except tritocerebral)
Non-neurosecretory neurons	10 ± 3	7 ± 2	0.7 – 1.0	All parts of CNS

Table 2. Histochemical responses of neurosecretory cells in *P. indicus*

Tests applied	Giant neuron			A – cell			B – cell			C – cell			REMARKS
	Cy	Nu	Nul	Cy	Nu	Nul	Cy	Nu	Nul	Cy	Nu	Nul	
1. Mercuric Bromophenol Blue test	+ + +	±	+ +	+ +	+	+ +	+ + +	+	+ +	+	±	+ +	Presence of general proteins
2. Ninhydrin-Schiff test	+	–	+	±	–	+	+	–	+	+	–	+	Presence of amino group
Deamination control	–	–	–	–	–	–	–	–	–	–	–	–	
3. Ferric-ferricyanide test	±	±	+	+	±	+	+	±	+	+	±	+ +	Presence of –SH groups
Mercaptide control	–	–	–	–	–	–	–	–	–	–	–	–	
4. Performic acid – alcian Blue test	+ + +	–	±	+	–	+	+ +	±	+	+	±	+	Presence of –S–S groups
Alcian blue alone-control	±	–	–	–	–	–	–	–	–	–	–	–	
5. Periodic acid Schiff test	+ +	–	±	+ + +	–	+	+ +	–	±	+	–	+	Presence of glycogen
Diastase digestion control	–	–	–	+	–	–	+	–	–	±	–	–	
6. Sudan Black B test	±	–	–	+	–	+	+ +	–	+	+ +	–	+	Presence of lipids
Delipidation control	–	–	–	–	–	–	–	–	–	–	–	–	
7. Methyl green pyronin test	±(R)	+(G)	±(R)	±(R)	+(G)	±(R)	+(R)	+(G)	+(R)	±(R)	+(G)	±(R)	Presence of RNA and DNA
10% perchloric control	–	–	–	–	–	–	–	–	–	–	–	–	
8. Alcian blue PAS test	+ +(M)	–	+(B)	+(M)	–	+(B)	+ +(M)	–	+(B)	No data			Presence of glycogen and mucopolysaccharides

Key: – Cy = Cytoplasm, Nu = Nucleus, Nul = Nucleolus, R = Pale Red, G = Green, M = Magenta, B = Blue, – = Negative reaction, ± = Very mild positive reaction of doubtful nature; + = Positive reaction; + + = Strong positive reaction; + + + = Intense positive reaction.

B cells

B cells were ubiquitous in all ganglia. Their shapes varied from oval to polygonal, but they are considerably smaller than GN and A cells and have relatively less cytoplasm (Table 1). These cells have round vesicular nuclei, with each cell possessing a single nucleolus measuring 3-4 μm in diameter (Fig. 2). B cells were always observed in groups of ten to twenty cells. Large numbers of vacuoles were noticed in these cells, and capillary plexuses and glial cells were observed in their pericellular regions. The perikarya showed an intense positive reaction to tests for the presence of general proteins and amino acids (Table 2). Further, B cell cytoplasm reacted in a strongly positive manner to the PAS test due to the presence of glycogen; only meagre amounts of lipids and RNA were found to be present in these cells.

C cells

These were the smallest NSCs observed, and were found in very limited numbers in all ganglia except tritocerebral ganglion. These cells were characterized by their pyriform shape, the narrow ends of which invariably continued as axons (Fig. 2). C cells have a single, centrally-placed and conspicuous nucleolus; the nucleus cytoplasm ratio was high due to the lesser amounts of cytoplasm contained within these cells (Table 1). C cells exhibit intense vacuole formation, and also have extracellular neuroglia and capillary networks. C cell cytoplasm reacted only moderately positive to proteins and carbohydrates tests, but showed a strong positive reaction to lipids (Table 2).

Apart from NSCs, many non-neurosecretory neurons were also observed in the ganglia; their dimensions are given in Table 1. These cells were considered non-neurosecretory because of their lack of stainable cytoplasm and the absence of observed changes in their perikarya.

Secretory cycle of NSCs

Cyclic changes were observed in the perikarya of the NSCs in relation to the synthesis of neurosecretory material. Among the different cell types we found no uniform patterns in the cyclic changes. Two morphological types of secretory cycles were observed, one common to GN and A cells and the other to B and C cells. However, the basic paterns of secretory cycles were essentially the same, involving three different phases: quiescent, vacuolar, and secretory. These phases were identified based on the appearance of secretory granules in the cytoplasm, vacuolization, and involovement of extracellular glial cells and capillary plexuses.

Quiescent (Q) phase

This is the resting or inactive phase of NSCs, within which the synthesis of secretory material is not apparent. Consequently, in all cell types the cytoplasm remained homogenous and lightly stained (Fig. 3). This phase is further characterized by the total absence of vacuoles in the cytoplasm and poorly stained glial cells and capillary plexuses.

Vacuolar (V) phase

NSCs in this phase have vacuoles in their perikarya. Vacuoles in GN and A cells vary widely in size and shape. In contrast, B and C cell vacuoles are fairly uniform in size and shape. Observed GN and A cell vacuoles ranged in size from 10 to 30 μm; interestingly, their shape varied from round or oval to a curious horseshoe shape (Fig. 4). These membrane-bound vacuoles are perinuclear in distribution and filled with a lightly-stained matrix. Cell cytoplasm is distinctly granular

and darkly stained, and peripheral glial cell nuclei are hypertrophied. (Fig. 4).

In observed B and C cells, the peripherally located membrane-bound vacuoles measured 10-15 μm in diameter, with their shape remaining consistently round or oval. Strangely enough, individual vacuoles tended to merge to form peripheral vacuolar rings around narrow bands of darkly stained perinuclear cytoplasm (Fig. 5). Hypertrophied glial cell nuclei (2 μm) and capillary plexuses were observed along the pericellular margins of B and C cells. The prominent nucleoli of these cells were observed in eccentric positions in the nuclei, and were occasionally seen in close contact with nuclear membranes (Fig. 5).

Secretory (S) phase

In this final phase of the secretory cycle, all observed NSC types were intensely stained; granular cytoplasm was interspersed with vacuoles. Vacuole diameters in GN and A cells decreased to 5-10 μm. Moreover, vacuoles migrated to peripheral regions from their previous perinuclear positions, and they contained darkly-stained granular material (Fig. 6). Also evident were hypertrophied glial cell nuclei (2-3 μm diameter) and capillary networks distributed randomly throughout the cells.

In B and C cells, the breadth and span of peripheral vacuolar rings became smaller; they were observed only as thin coverings around the cytoplasm (Fig. 7). Vacuole size also diminished to approximately 5 μm. The cytoplasm during this phase appeared frothy due to the random dispersion of secretory granules. Glial cells and capillary networks were also seen around B and C cells.

Distribution and Mapping of NSCs

Eyestalk

The eyestalk of *P. indicus* is composed of several neural structures, the microanatomy of which was found to be rather complex. A schematic representation of the left eyestalk indicating the positions of the medullary lobes, X-organs, and sinus gland is given as Fig. 8. NSCs in the eyestalk were found in three conspicuous groups and, based on their location, named as medulla terminalis ganglionic X-organs 1 and 2 (mtgxo 1 and 2) and medulla externa ganglionic X-organ (megxo). NSCs were not observed in the lamina ganglionaris (1g) and medulla interna (mi).

The principal NSC groups were found on the apical surface of the mt lobe. In the left eyestalk, the group on the left was termed mtgxo-1 and the group on the right mtgxo-2. The pyriform mtgxo-1 has a large number of B cells, a few C cells, and two or three A cells (Fig. 9). On the other hand, the mtgxo-2 group was roughly elliptical in shape with a large number of B and C cells. A single A cell was observed on the dorsal side of this X-organ. The megxo was observed on the lateral surface of the me, on its rostral side. This group was observed to be diffuse, with a number of B and C cells found on both dorsal and ventral surfaces. Two or three A cells were also seen on the ventral side at the proximal extremity of the lobe. (Fig. 11)

The neurohemal organ sinus gland (sg) was always found to be associated with one of the finger-like vascular processes (external blood sinuses) found around the medullary lobes. In the left eyestalk, the sg was located on the left side – in the space between the me and mi lobes. The sg has an elliptical shape and is flattened dorsoventrally. The central part of the gland is occupied by an internal blood sinus. Swollen axonal endings and granular aggregations were frequently observed in the sg (Fig. 10). The nervous tract from the X-organs (X-organ-sinus gland tract) was observed infrequently and never in its entirety, but is nevertheless presented

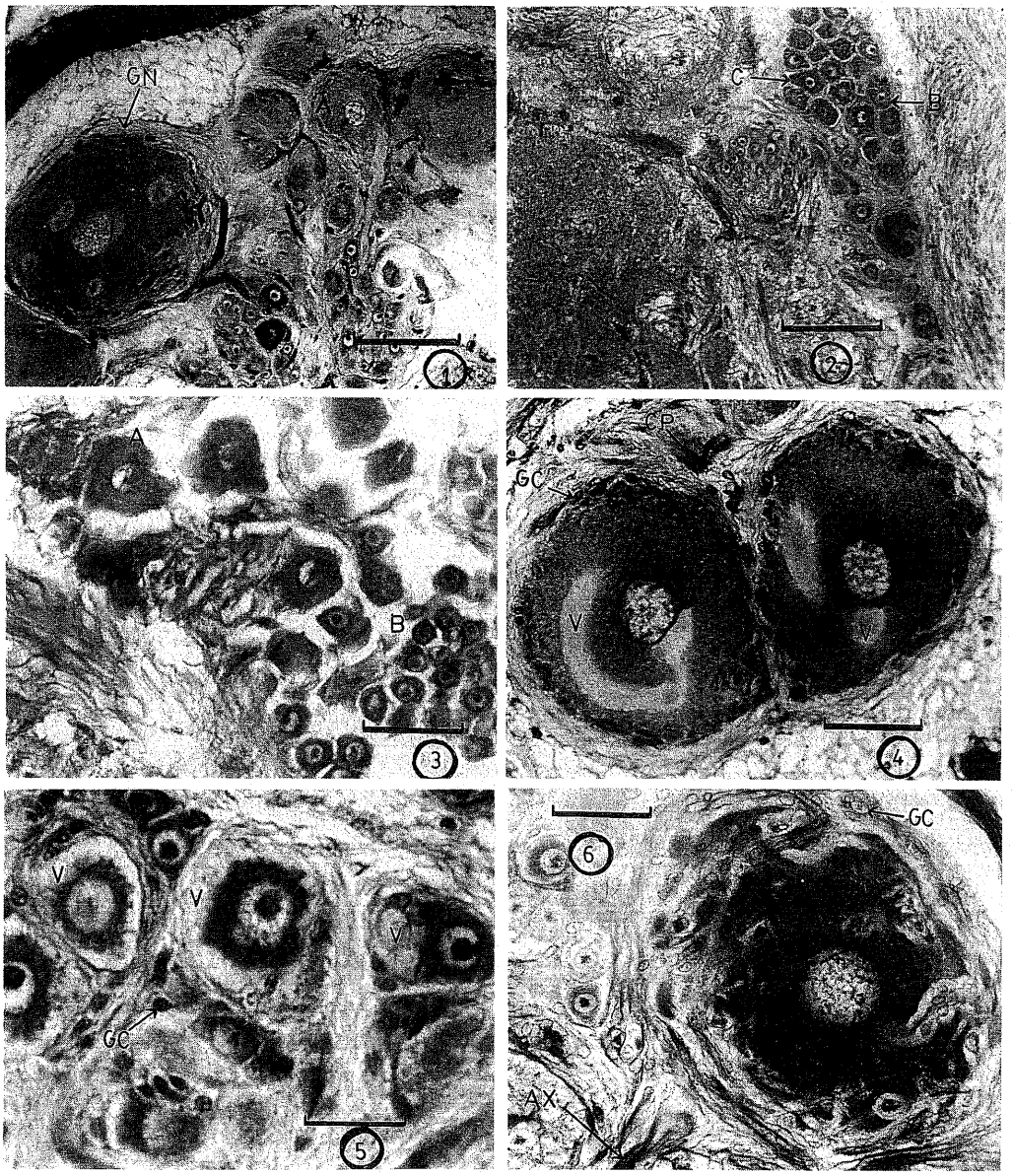

Fig. 1. GN and A cells in subesophageal ganglion. Note the vacuolated cytoplasm as well as the axon leaving the NSC. Bar equals 50 μm.

Fig. 2. B and C cells in subesophageal ganglion. Bar equals 100 μm.

Fig. 3. Quiescent phase A, B, and C cells in the MEGXO. Bar equals 50 μm.

Fig. 4. Vacuolar phase GN cells in thoracic ganglion. Note the large perinuclear vacuoles (V), glial cells (GC), and capillary plexus (CP) around the NSC. Bar equals 25 μm.

Fig. 5. Vacuolar phase B and C cells in supraesophageal ganglion. Vacuoles (V) originate in the peripheral regions of the cell and later coalesce to form a large pericellular vacuole. Also note the hypertrophied glial cells (GC) auound the NSCs. Bar equals 25 μm.

Fig. 6. GN cell in its terminal phase with peripheral vacuoles containing neurosecretory granules and hypertrophied neuroglia (GC). Axon (AX) is also deeply stained. Bar equals 25 μm.

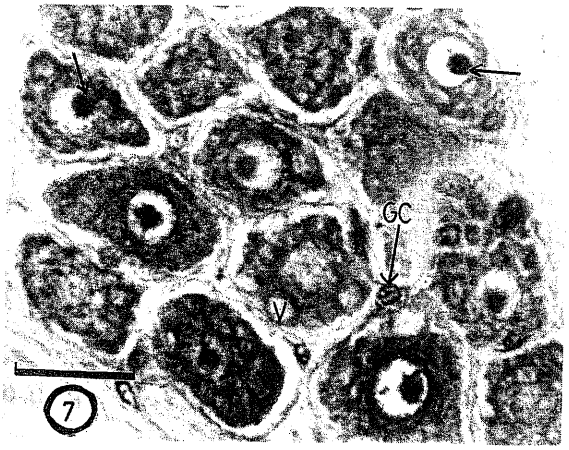

Fig. 7. Secretory phase B and C cells in subesophageal ganglion. Note the extremely granular and frothy nature of the cytoplasm interspersed with vacuoles (V). The nucleolus is eccentric in its position, and glial cells (GC) are hypertrophied. Bar equals 25 μm.

Fig. 9. The pyriform MTGXO-1 with A, B, and C cells. Note the combined axons leaving the X-organ. Bar equals 50 μm.

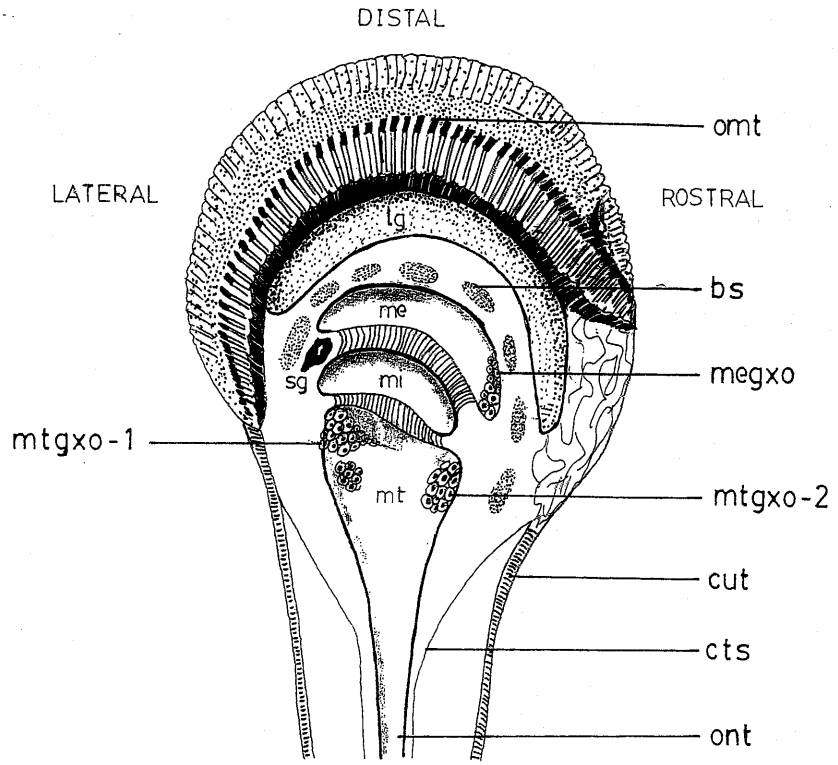

Fig. 8. Schematic representation of the important structures in the left eyestalk as seen from the dorsal side. Key: omt – ommatidia, lg – lamina ganglionaris, bs – blood sinus, me – medulla externa, megxo – medulla externa ganglionic X-organ, sg – sinus gland, mi – medulla interna, mt – medulla terminalis, mtgxo-1 – medulla terminalis ganglionic X-organ one, mtgxo-2 – medulla terminalis ganglionic X-organ two, cut – cuticle, cts – connective tissue sheath, and ont – optic nerve tract.

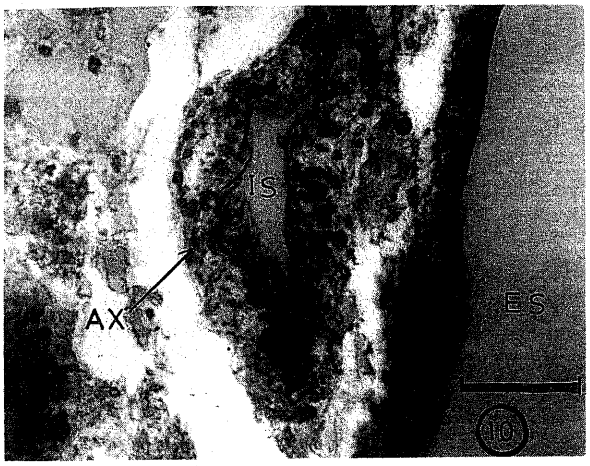

Fig. 10. Detail of the sinus gland adjacent to the external blood sinus (ES). Note the abundance of neurosecretory granules, bulbous axonal endings (AX), and the internal blood sinus (IS). Bar equals 25 μm.

schematically in Fig. 11.

Supraesophageal ganglion

The NSC groups are distributed in the peripheral regions immediately underneath connective tissue sheaths. A total of eleven NSC groups — six on the ventral side and five on the dorsal side — were identified and named according to their location (Fig. 12). The observed pairs of anterior and posterior dorsal groups and anterior and posterior ventral groups mostly contained A and B cells, whereas C cells were found exclusively in the anterior ventral group. A pair of median ventral groups were also found to have only A and B cells. The central dorsal group observed in the middle of the ganglion was the largest, having a large number of GN cells.

Tritocerebral ganglion

This extremely small ganglia, which lies midway between the tritocerebral connectives, is characterized by the presence of two exceptionally large GN cells; apart from these, several B cells and one A cell were also seen on its lateral side (Fig. 13).

Subesophageal ganglion

A maximum number of fifteen NSC groups were observed in this ganglion on its dorsal, dorso-median, and ventral sides (Fig. 13). The dorsal aspect of this ganglion reveals three dorso-median cell groups (DMG) termed as DMG I, II, and III. Occupying the anterior position, DMG I was observed as the largest, with only GN and A cells; DMG II and III are smaller, with only B and C cells. In the dorso-middle plane, eleven dorso-lateral groups (DLG) with B and C cells were seen. Ventrally, this ganglion had only one elongated ventromedian group (VMG), comprised exclusively of GN and A cells.

Thoracic ganglion

Distributions of NSCs in all thoracic ganglia were similar. Dorsally, three NSC groups were observed, with one pair at the anterior end termed as the anterior dorsal group (ADG) and another at the posterior end termed as the posterior dorsal group (PDG). The ADG and PDG contain few A and C cells and a comparatively higher number of B cells (Fig. 14). Ventrally, we found a single oblong ventromedian group (VMG) which had only GN and A cells.

Abdominal ganglion

These ganglia were found to be poor in NSC groups. A pair of anterior and posterior lateral groups (ALG and PLG) were observed on both dorsal and ventral sides of these ganglia (Fig. 14). Both ALG and PLG had A, B, and C cells; GN cells were absent.

Ultrastructural investigations of the NSCs revealed the presence of electron-dense neurosecretory granules in their perikarya. These granules, which varied in size from

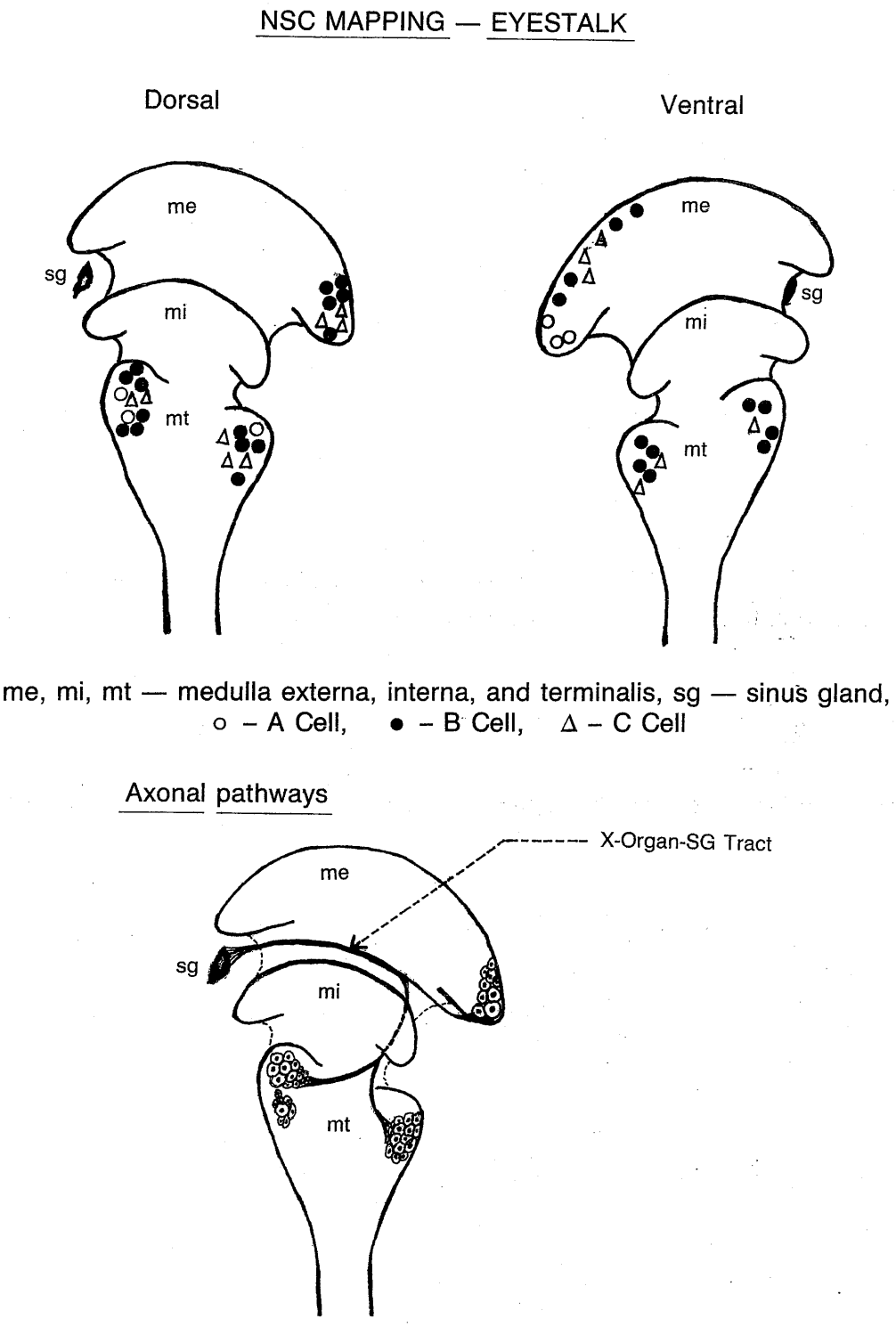

Fig. 11. Distribution and mapping of NSCs in the eyestalk and the axonal pathways from the X-organs to the sinus gland.

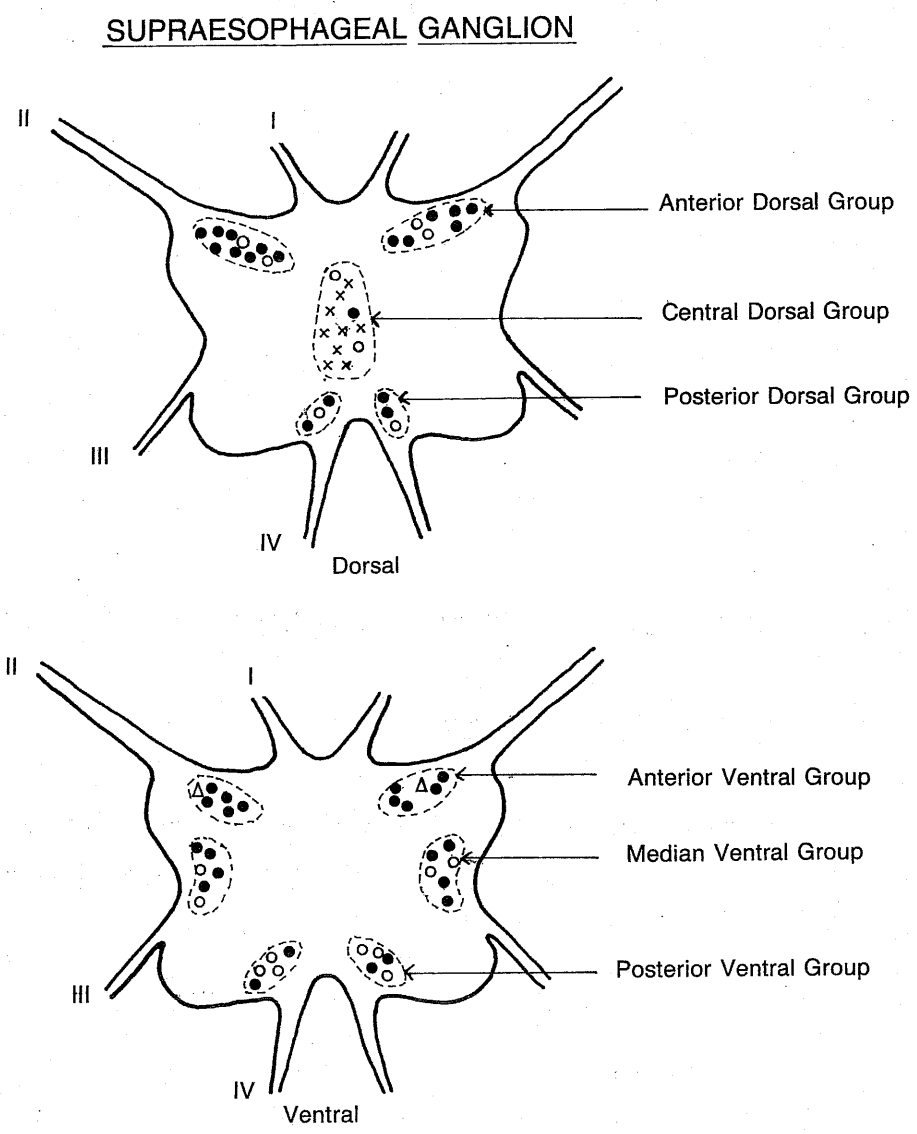

Fig. 12. Distribution and mapping of NSCs in the supraesophageal ganglion.
Key: I – Antennary nerve; II – Optic nerve; III – Maxillary nerve; IV – Circumesophageal connective; x – GN cell; o – A cell; • – B cell; Δ – C cell

1,400 to 1,600 Å, were enveloped within single smooth membranes and contained electron-dense material which was separated from the membrane by less electron-dense halos (Fig. 15). Differences in the electron densities of the granules were noted. Some of the observed granules showed high degrees of electron density, were finely granulated, and were also homogenous. A second granule type was seen to be moderately electron dense and coarsely and loosely granulated.

DISCUSSION

NSCs in *P. indicus* were found to be distinct from nerve cells; the characteristics

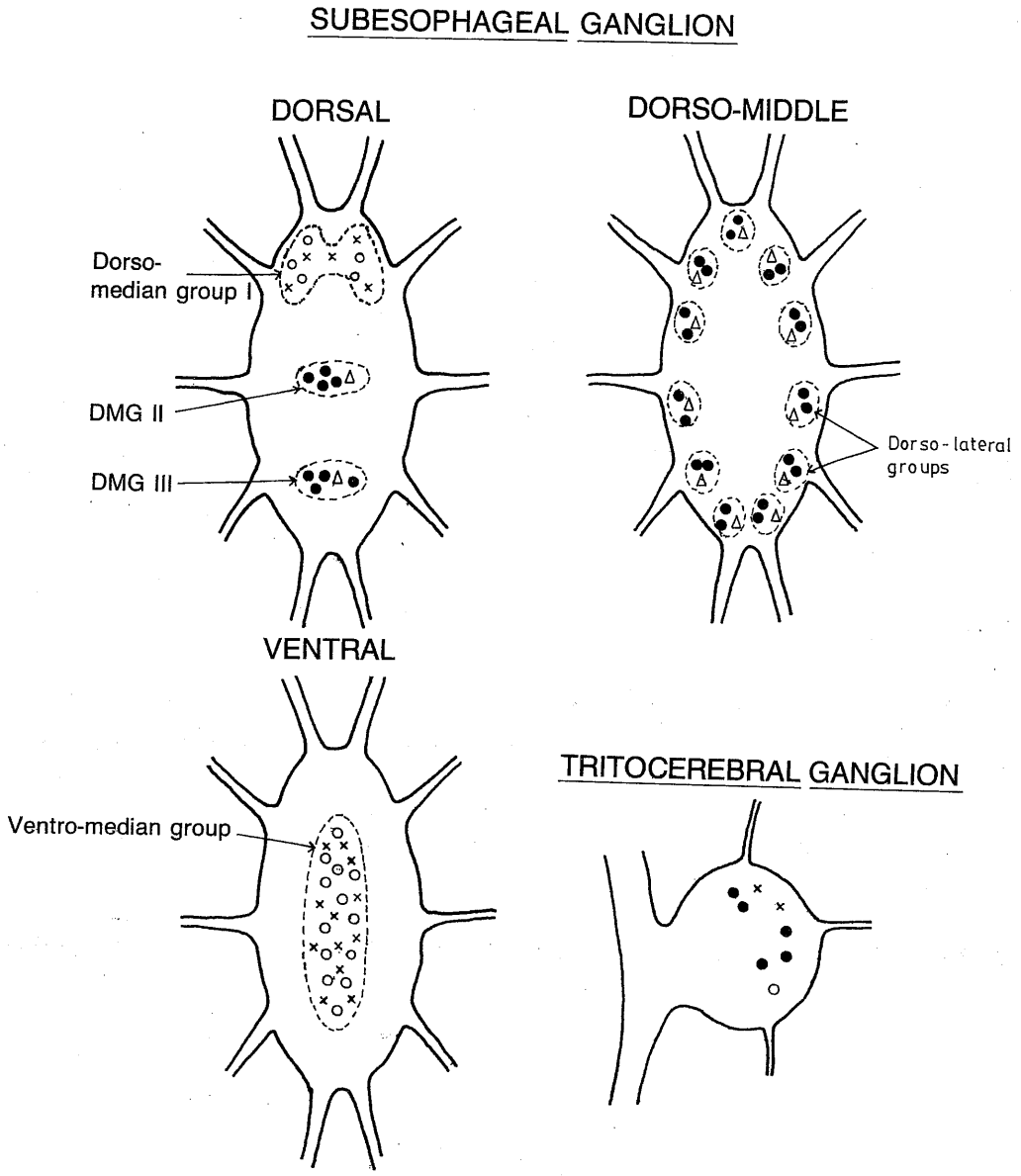

Fig. 13. Distribution and mapping of NSCs in the subesophageal and tritocerebral ganglion. Key: x – GN cell; o – A cell; • – B cell; Δ – C cell

we observed are basically in accord with those of neurosecretory elements described in other crustaceans by many researchers (Enami, 1951; Durand, 1956; Matsumoto, 1958; Lake, 1970; Nakamura, 1974; Van Herp *et al.*, 1977).

Descriptions of NSC types found in different penaeid species are probably varied because of differences in staining techniques, cyclic secretory activities, species differences, and human subjectivity. Thus, seven NSC types were described by Nakamura (1974) in *P. japonicus,* four in *P. monodon* by Nanda and Ghosh (1985), and eight in *Parapenaeopsis stylifera* by Nagabhushanam *et al.* (1986). The four NSC

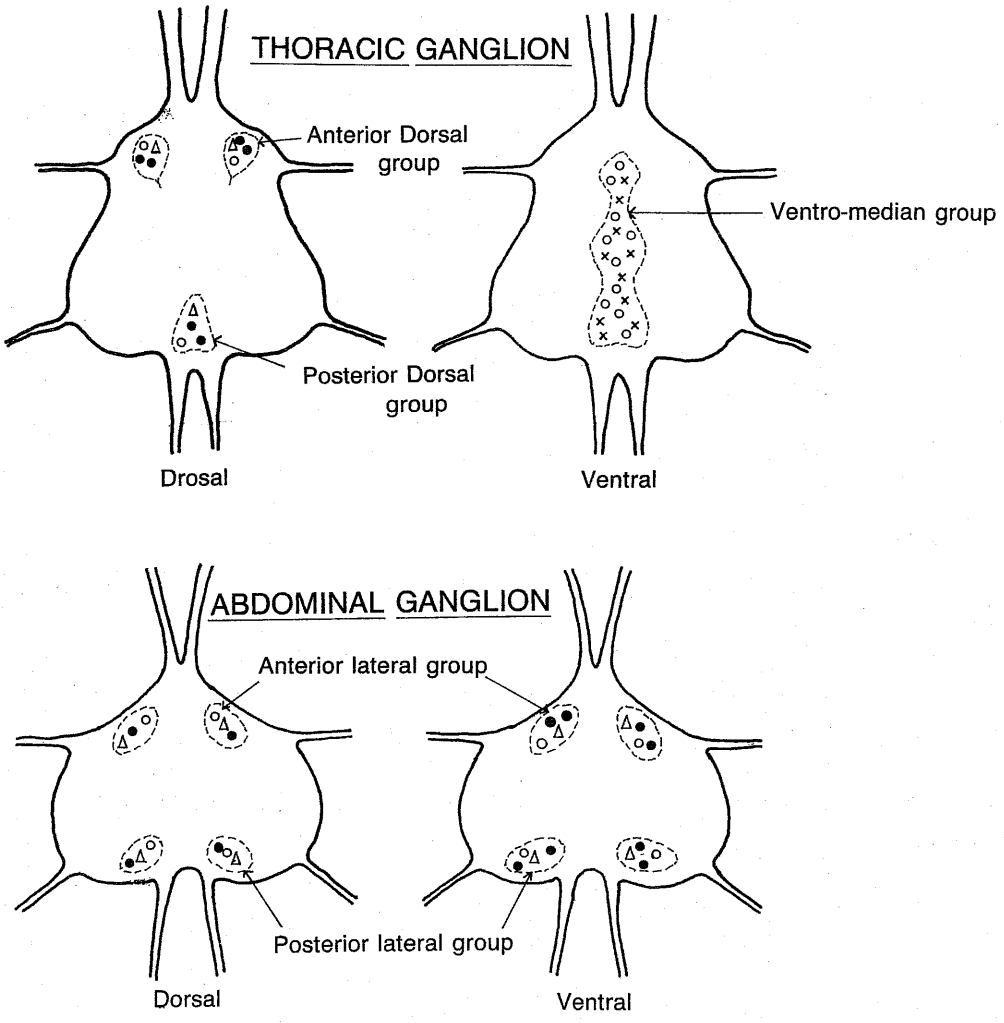

Fig. 14. Distribution and mapping of NSCs in the thoracic and abdominal ganglion. Key: x – GN cell; o – A cell; • – B cell; Δ – C cell

types found in *P. indicus* seems to be a relatively larger number than those described in other penaeid species, although they are comparable in shape and histological features.

Almost all previous investigators referred to the small nerve cells (which are designated as non-neurosecretory in this study) as neurosecretory because of their appearance amidst NSC groups. However, these cells did not show any neurosecretory activity in the present study and hence they were not given neurosecretory status — even though the cells are comparable to cell types V and VI of *P. japonicus* (Nakamura, 1974) and type VIII of *P. stylifera* (Nagabhushanam *et al.*, 1986).

The neurosecretory material contained in the NSCs of *P. indicus* was predominantly composed of a protein rich in cystine (-S-S group) and cysteine (-SH group). Being a storage site in the eyestalk, the sinus gland

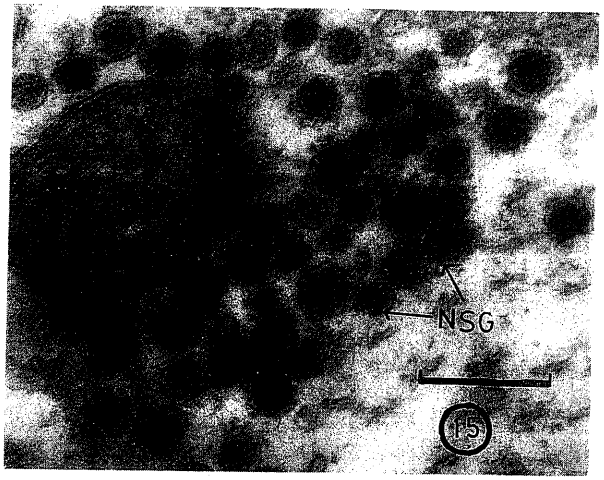

Fig. 15. Electron micrograph of an NSC perikarya in the optic ganglia indicating electron dense neurosecretory granules (NSG). Bar equals 0.5 μm.

also showed similar characteristics. The neurosecretory material in other crustaceans (Lake, 1970) and some insects (Raabe, 1980) was also reported to be rich in sulphur-containing amino acids. Recent studies on the biochemistry of crustacean neurohormonal peptides have indicated that the amino acid cystine is one of the components of crustacean hyperglycemic hormone (GHH), moult inhibiting hormone (MIH) and crustacean cardioactive peptide (Webster and Keller, 1988). Nakamura (1974) referred to the NSCs in *P. japonicus* as 'PAS positives' because of their strong positive reactions to PAS tests. In our study, however, PAS reaction was only moderate.

Cyclic secretory activity is indicative of the neurosecretory status of a nerve cell. In *P. indicus,* two morphologically diverse secretory cycles were observed; these have been correlated with the processes of moulting (Vijayan, 1988) and reproduction (Mohamed and Diwans, 1991). Among crustaceans, only few researchers (Enami, 1951; Matsumoto, 1958; Williams *et al.,* 1980; Chandy and Kolwalker, 1985) have discussed the secretory activities of NSCs in detail, and most of them have noted the formation of peripheral vacuoles as indicative of the terminal phase in the secretory cycle. In *P. indicus,* vacuole formation is the first phase in the activation of the cell for synthesis of neurosecretory material; in general, vacuole size diminishes with heightened secretory activity when granular inclusions also increase. The role of neuroglia in the NSC secretory cycle of *P. indicus* appears to be unique, although some indications of glial activity was reported by Lake (1970) in the brains of the crab *Paragrapsus gaimardii.* The glial cells surrounding the NSCs become hypertrophied during the V and S phases. For the most part, the glio-neuronal relationship in crustaceans is vague, although glial cells may serve as sources of nutritive material during the synthetic phase of NSCs. More significantly, they may also serve as a media between an NSC and its surrounding capillary network, thus forming a glio-vascular relationship similar to that existing in vertebrates (Glees and Meller, 1968).

The major structural components of the penaeid eyestalk are apparently similar, but controversy exists with regard to NSC groups associated with the medullary lobes. For instance, some studies (such as the present one) do not recognize the migx organ (Nakamura, 1974; Nanda and Ghosh, 1985) while others do (Dall, 1965). This discrepancy is perhaps a function of identifying or associating an NSC group with a particular medullary lobe. The observation of three cell types in the mtgxo and megxo of *P. indicus* corroborates observations reported in *Palaemon serratus* (Van Herp *et al.,* 1977) and *P. japonicus* (Nakamura, 1974). The sinus gland of *P. indicus* — which has swollen axonal endings, granular aggregations, and an internal blood sinus — is similar in structure and position to the sinus gland of *P. serratus* (Van Herp *et al.,* 1977).

In comparison to the eyestalk, NSC groups in other parts of the central nervous

system have only been sparingly investigated in penaeids. Nakamura's (1974) studies of *P. japonicus* revealed eight NSC groups in the supraesophageal ganglion in contrast to the eleven groups observed in the present study. However, those regions where NSCs occur in the brain of *P. indicus* are similar to those observed in *P. japonicus* (Nakamura, 1974) and *P. stylifera* (Negabhushanam *et al.*, 1986). Surprisingly, with regard to the remaining ventral ganglia there are no comparable studies for penaeids. In pleocyematans, these ganglia have been fairly well studied, probably because all of the ganglia in the thorax have fused to form a single thoracic ganglion. However, in dendrobranchiates such as penaeids, each somite is represented by a ganglion. The most striking feature in the distribution of NSCs in *P. indicus* is the total absence of GN cells in the eyestalk despite their dominance in almost all of the ventral ganglia.

Fine structure studies of the neurosecretory material in *P. indicus* have shown haloed dense-core granules with narrow diameters. However, *P. japonicus,* Nakamura (1980) observed granules with wider diameters of 1,100 to 1,900 Å. The presence of granules with different electron densities was also reported in *Carcinus maenas* by Smith (1975).

Acknowledgements: We are grateful to Dr. P. S. B. R. James, Director, and Dr. E.G. Silas, former Director of the Central Marine Fisheries Research Institute, Kochi for providing facilities and encouragement. We are also grateful to the Indian Council of Agricultural Research, New Delhi for financial support during the research.

REFERENCES

Adiyodi KG, RG Adiyodi. 1970. Endocrine control of reproduction in decapod Crustacea. Biol. Rev. **45:** 121-165.

Chandy JP, DG kolwalker. 1985. Neurosecretion in the marine crab Charybdis lucifera. Indian J. Mar. Sci. **14:** 31-34.

Dall W. 1965. Studies on the physiology of a shrimp *Metapenaeus* sp. II. Endocrines and control of moulting. Australian J. Mar. Fresh. Res. **16:** 1-12.

Durand JB. 1956. Neurosecretory cell types, their secretory activity in the crayfish. Biol. Bull. (Woods Hole). **111:** 62-76.

Enami M. 1951. The sources and activities of two chromatophoro-tropic hormones in crabs of the genus *Sesarma*. II. Histology of incretory elements. Biol. Bull. (Woods Hole). **101:** 241-258.

Glees P, K Meller. 1969. Morphology of neuroglia. *In* The structure and function of nervous tissue. Vol. I (G. H. Bourne, ed.) Academic Press, New York. pp. 301-323.

Kurup NG. 1972. Staining techniques of the neuroendocrine tissues of decapod Crustacea. *Hydrobiol.* **40:** 87-100.

Lake PS. 1970. Histological and histochemical observations of the cephalic neurosecretory systems of the crab *Paragrapsus gaimardii* (Milne Edwards). Proc. Royal Soc. Tasmania **105:** 87-96.

Matsumoto K. 1958. Morphological studies on neurosecretion in crabs. Biol. J. Okayama Univ. **4:** 103-176.

Mohamed KS, AD Diwan. 1991. Neuroendocrine regulation of ovarian maturation in the Indian white prawn *Penaeus indicus.* H Milne Edwards. Aquaculture **98:** 381-393.

Nagabhushanam R, R Sarojini, PK Joshi. 1986. Observations on the neurosecretory cells of the marine penaeid prawn, *Parapenaeopsis stylifera*. J. Adv. Zool. **7:** 63-70.

Nakamura K. 1974. Studies on the neurosecretion of the prawn *Penaeus japonicus* B. I. Positional relationships of the cell groups located on the supraesophageal and optic ganglions. Mem. Fac. Fish. Kagoshima Univ. **23:** 173-184.

Nakamura K. 1980. Electron microscopical observation of the PAS positive cells in the supraesophageal ganglion of the prawn, *Penaeus japonicus* B. J. Japanese Soc. Sci. Fish. **46:** 1211-1215.

Nanda DK, PK Ghosh. 1985. The eyestalk neurosecretory system in the brackish water prawn, *Penaeus monodon* (Fabricius). A light microscopical study. J. Zool. Soc. India. **37:** 25-38.

Pearse AGE. 1968. Histochemistry, Theoretical and applied Vol. I. Churchill Livingstone, London. 759 pps.

Raabe G. 1980. Some remarks concerning staining methods for neurosecretory products in insects. Experientia (Basel). **36:** 1237-1238.

Smith G. 1975. The neurosecretory cells of the optic lobe in Carcinus maenas (L). Cell Tiss. Res. **156:**

403-409.
Van Herp F, C Bellon-Humbert, JTM Luub, A Van Wormhoudt. 1977. A histophysiological study of the eyestalk of *Palaemon serratus* with special reference to the impact of light and darkness. Arch. Biol. **5:** 257-278.
Vijayan KK. 1988. Studies on the physiology of moulting in the penaeid prawn, *Penaeus indicus*. PH.D. thesis, Cochin University, Kerala. 265 pp.
Webster SG, R Keller. 1988. Physiology and biochemistry of crustacean neurohormonal peptides. *In* Neurohormones in Invertebrates (MC Thorndyke, GJ Goldsworthy, eds.). Cambridge University Press, Cambridge, New York. pp. 173-196.
Williams JA, RSV Pullin, E Naylor, G Smith, BG Williams. 1980. The role of Hanstrom's organ in clock control in *Carcinus maenas*. *In* Cyclic phenomena in marine plants and animals (E Naylor, RG Hartnoll, eds.). Pergamon Press, New York. pp 459-468.

印度白對蝦（*Penaeus indicus*）神經內分泌系統的組織形態學報告

K. Sunilkumar Mohamed, K.K. Vijayan and A.D. Diwan

印度白對蝦（*Penaeus indicus*）的神經內分泌系統經由光學顯微鏡及穿透式電子顯微鏡的檢視下，發現了其神經內分泌細胞有四種不同的形態，分別是巨神經細胞 (GN) 及 A、B、C 型四種形態。本文描述了這些細胞的特質及其組織化學的特性。所有的神經內分泌細胞都表現出一種週期性的分泌活性，而且可由其染色的微粒、液泡及膠質細胞的出現順序來區別三個不同的時期。另外，分布在眼柄、腦、後腦及食道下神經節、胸、腹神經節的神經內分泌細胞都已繪製成圖。眼柄的X器官沒有GN細胞的存在，但在其他的神經節中卻包含很多GN細胞。這些神經內分泌物質被發現是一個直徑 1400 Å 到 1600 Å 且呈光環狀的小微粒。

Bull. Inst. Zool., Academia Sinica **32**(1): 54-61 (1993)

Spotlight counts of giant flying squirrels (*Petaurista petaurista* and *P. alborufus*) in Taiwan

PEI-FEN LEE,[1] DONALD R. PROGULSKE[2] and YAO-SUNG LIN[1]

[1]*Department of Zoology, National Taiwan University, Taipei, Taiwan 10764, Republic of China*

and

[2]*Department of Forestry and Wildlife Management University of Massachusetts, Amherst, MA 01003, U.S.A.*

(Accepted June 2, 1992)

We studied population trends for two sympatric flying squirrels (*P. petaurista* and *P. alborufus*) via night spotlight counts from October, 1981 to August, 1984 in Chitou, Taiwan. A total of 298 *P. petaurista,* 281 *P. alborufus,* and 2,722 calls (337 *P. petaurista,* 2,385 *P. alborufus*) were recorded over 107 nights. Monthly mean densities (squirrels/10 ha) of *P. petaurista* and *P. alborufus* observed in hardwood forests were significantly higher than those observed in conifer plantations ($p < 0.01$). In hardwood forests, *P. alborufus* were equally abundant as *P. petaurista,* but in conifer plantations the latter was significantly more abundant than the former ($p < 0.001$). *P. alborufus* densities in hardwood forests showed seasonal differences ($p < 0.001$), with the highest in fall ($\bar{x}$ = 4.2 squirrels/10 ha, SE = 0.08) and the lowest in winter ($\bar{x}$ = 2.2 squirrels/10 ha, SE = 0.19); the *P. petaurista* populations in both habitats showed no seasonal variations. *P. petaurista* densities observed in hardwood forests were positively correlated with those of *P. alborufus* in the same habitat, but no correlations were found in the other situation. Call indexes for both species did not correlate with the estimated densities.

Keywords: Giant flying squirrel, *Petaurista,* Population trend.

Giant flying squirrels (*Petaurista* spp.) have the highest diversity in terms of species richness and population density in southeast Asia (Honacki *et al.* 1982). Five species have been recognized: *P. alborufus, P. elegans, P. leucogenys, P. magnificus,* and *P. petaurista* (Nowak and Paradiso 1983). Among these, only the ecology of *P. leucogenys* has been extensively studied in Japan (e.g., Baba 1978, Ando and Imaizumi 1982, Baba *et al.* 1982, Ando *et al.* 1983, 1984, Ando and Shiraishi 1983, 1984). No study has been made on the population trends of giant flying squirrels.

Taiwan has two *Petaurista* species: the Formosan red-giant flying squirrel (*P. petaurista*) and the Formosan white-headed flying squirrel (*P. alborufus*) (Jones *et al.* 1971). Both species are arboreal folivores which rely on forest habitat (Muul and Lim 1978, Lee *et al.* 1986). They primarily use tree cavities as nests during the daytime. Previous studies have revealed that these two species do not overlap in their distributions (Kano 1940); however, Lee *et al.* (1986) recently found that both species live sympatrically in mountain forests at elevations